

# Transition Dynamics and Confinement Scaling in COMPASS-D H-mode Plasmas

S.J. Fielding, P.G. Carolan, J.W. Connor, N.J. Conway, A.R. Field, P. Helander, Yu Igitkhanov 1), B. Lloyd, H. Meyer, A.W. Morris, O. Pogutse, M. Valovic, H.R. Wilson and the COMPASS-D & ECRH Teams

EURATOM/UKAEA Fusion Association, Culham Science Centre, Abingdon, Oxfordshire, OX14 3DB, UK

1) ITER Joint Central Team, Joint Work-Site, D-85748 Garching, Germany

e-mail contact of main author: [steve.fielding@ukaea.org.uk](mailto:steve.fielding@ukaea.org.uk)

**Abstract** This paper describes experimental analysis of different phases of ECRH H-mode discharges on COMPASS-D, from L-H transition trigger to steady state. Comprehensive high-resolution measurements of the transport barrier region have enabled significant progress to be made in assessing H-mode trigger mechanisms, as well as clarifying the evolution of the local electric field and its shear. Stationary ELMy H-modes are achieved at high  $\rho^*$  with good confinement, and dimensionless scaling over a range of  $\nu^*$  is presented.

## 1. Introduction

COMPASS-D is a compact tokamak ( $R=0.56\text{m}$ ,  $a=0.17\text{m}$ ,  $\kappa\leq 1.7$ ,  $\delta\leq 0.4$ , ECRH: 60GHz,  $\leq 1.5\text{MW}$ ) achieving clear H-modes and providing key scaling data for ITER-like devices. We describe here experimental analysis of different phases of the H-mode discharge on COMPASS-D, from L-H transition trigger to steady state. High-resolution edge measurements encompassing the transport barrier have enabled significant progress to be made in assessing proposed H-mode trigger mechanisms, and allow the evolution of the local electric field and its shear to be evaluated.

COMPASS-D can routinely generate stationary ELMy H-modes with ECRH, in relevant high triangularity configurations. Such plasmas extend confinement databases towards large values of normalised Larmor radii where L-mode (Bohm) and H-mode (gyro-Bohm) energy confinement scalings predict interestingly very close values. These plasmas can also be used for dimensionless-scaling experiments and results displaying a factor-of-five range in collisionality are reported here.

## 2. H-mode transition trigger

Thermal helium beam spectroscopy provides profiles of  $T_e$  and  $n_e$ ,  $T_i^{Imp}$ , plasma rotation and radial electric fields in the plasma boundary ( $\Psi_N \sim (r/a)^2 \geq 0.9$ ) [1] and the stability of the H-mode transport barrier is assessed in terms of the behaviour of normalised parameters evaluated from these measurements [2]. In Fig.1(a) plots of normalised edge electron pressure gradient,  $\mathbf{a}_e = Rq^2 db/dr$  against edge collisionality,  $\mathbf{n}_e^*$  show that H-mode is confined to a region where both  $\mathbf{a}_e$  and  $\mathbf{n}_e^*$  exceed critical values. L-H transition points lie on or close to these boundaries, consistent with stabilisation of the peeling mode [3] as a necessary condition for H-mode.

Three-dimensional, non-linear simulations of drift-ballooning modes [4] indicate that electromagnetic fluctuations significantly enhance transport when  $\mathbf{a}_e$  exceeds a critical value well below the ballooning limit, unless diamagnetic effects are strong. For  $\alpha_e > 0.5$  strong sheared poloidal flow develops, driven by non-linear Kelvin-Helmholtz instability, when the

normalised diamagnetic parameter  $\mathbf{a}_{dia} = (2pq)^{-1} (m_i / 2m_e)^{1/4} (v_{th,e} / n_{ei} \sqrt{RL_n})^{1/2} > 0.75$ . This suppresses turbulent transport. Fig. 1(b) shows that there is a critical  $\mathbf{a}_e$  for the occurrence of H-mode but no evidence for a correlation with

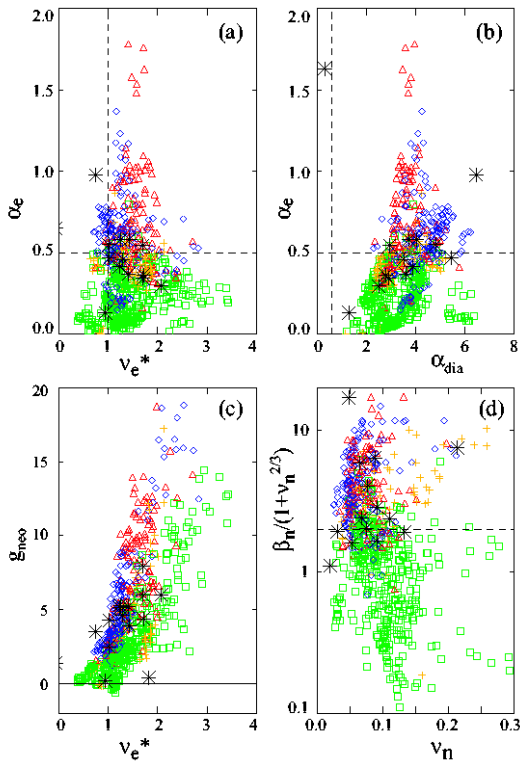


Fig. 1 Stability plots for various theories of edge instabilities and transport: (a) Peeling mode; (b) drift-ballooning; (c) neo-classical transport bifurcation; (d) Alfvén-drift wave turbulence suppression. Points are during L-mode (squares), ELM-free (triangles), ELMy (diamonds), dithering H-mode (crosses) and L-H transition (stars) and refer to the 90% flux surface.

frequency. Fig. 1 (d), a plot of  $\mathbf{b}_n / (1 + \mathbf{n}_n^{2/3})$  against  $\mathbf{n}_n$  for COMPASS-D, reveals a critical value  $\approx 2$ , at the L-H transition and data from dithering sections of the L-H transition are clearly separated from L-mode data. This ‘precursor’ behaviour indicates that suppression of this turbulence occurs particularly early in the transition evolution and may act as a controlling trigger. This mechanism is also consistent with data from a wide range of tokamaks and can be formulated to predict the differences in the L-H power threshold observed between COMPASS-D and other devices. In particular, the predicted scaling in COMPASS-D  $P_{th} \mu B^3 / n^{1.5}$  agrees closely with that observed  $P_{th} \mu B^{3.6} / n^{1.5}$  [2].

More directed experimentation is required to resolve which particular mechanism controls the L-H transition. To test whether the peeling mode may be limiting access to H-mode at low density on COMPASS-D, current ramps have been generated in discharges close to the L/H-transition threshold [7]. Observations are that current ramp-up, with increased edge current, hence increased peeling mode drive, triggers a transition to H-mode, current ramp-down discharges remain in L-mode. This is opposite behaviour to that expected if the peeling mode controlled the transition. A schematic criterion for peeling stability is given by

$\mathbf{a}_{dia}$ .

A bifurcation in the underlying neo-classical transport, with a reduction in radial particle transport, may occur with sufficiently steep edge gradients. An extension of neo-classical theory of an impure plasma [5] into such regimes predicts that as  $r_{iq}/L^\wedge$  increases ( $L^\wedge =$  pressure radial scale length) a poloidal asymmetry should develop in the impurity density. This reduces the parallel impurity-ion friction and the radial particle flux, provided that  $g_{neo}$  (a normalised parameter characterising edge gradients) exceeds a critical value  $\approx 2$ . As shown in Fig. 1 (c), assuming  $T_e=T_i$  and a representative impurity of  $Z=5$ , there is evidence of a critical  $g_{neo} \sim 2-5$  for formation of the H-mode on COMPASS-D.

Recent theoretical studies of Alfvén-drift wave turbulence suppression [6] indicate that as the edge electron diamagnetic-drift velocity

increases, interaction between electron drift waves and Alfvén waves can suppress the long wavelength drift-waves thought to be responsible for edge transport. The criterion for turbulence suppression is  $\mathbf{b}_n > 1 + \mathbf{n}_n^{2/3}$ , where  $\mathbf{b}_n = (M/m)^{1/2} \mathbf{a}/sq$ ,  $s$  is the shear ( $rq'/q$ ) and  $\mathbf{n}_n$  is a normalised electron collision

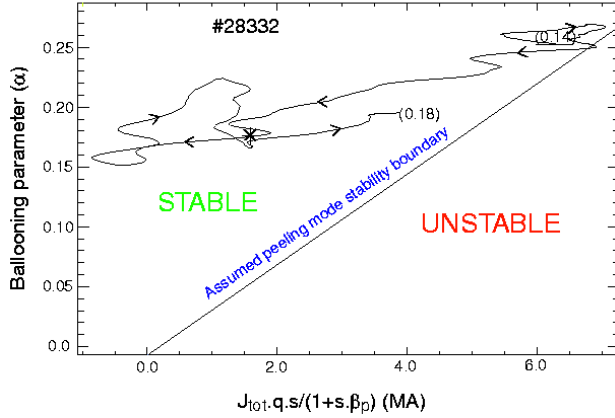


Fig.2 Schematic peeling mode stability diagram for current ramp-down discharge. The stability boundary is assumed to lie just below the experimental values at 0.14s, when the discharge is just in H-mode. Arrows indicate the direction in time and the asterisk denotes the H-L transition.

is observed to evolve into H-mode. These experiments indicate that the peeling mode is not having a controlling influence on the H-mode transition under these conditions, the plasma being peeling stable in both L- and H-mode. Peeling mode stability may however still be a necessary condition for attainment of H-mode and this instability may play a role in the formation of ELMs [8].

Current ramps at high density with Ohmic heating, show the opposite behaviour – current ramp down at threshold conditions leads to a clear confinement improvement [9]. Similar results have also been observed on devices which report power thresholds in agreement with ITER scalings eg JET [10]. At these high density conditions on COMPASS-D the estimated power threshold also agrees with ITER scalings, indicating that in this regime the transition controlling mechanisms may be similar to those on other devices, and different to that in low density ECRH discharges.

### 3. Transport barrier evolution

Poloidal velocities are measured using high resolution Doppler spectroscopy,  $\Delta t = 2.5\text{ms}$ ,  $\Delta r = 2\text{mm}$ . Fig 3 shows the evolution of the poloidal velocity on surfaces of constant poloidal flux, during a series of triggered confinement transitions [11]. Significant velocity shear only evolves after the L-H transition, with a maximum in H-mode around the 93% flux surface. Gas puff at 170ms initiates a decay in the shear, leading to an H-L transition when the shear is virtually removed. In the subsequent L-mode phase the rotation is rapidly suppressed. The second L-H transition is initiated when the gas puff is again turned off and the poloidal velocity and its shear increase as before. We compute the radial electric field from the radial impurity momentum balance, ignoring contributions from inertia, friction and viscosity, and toroidal velocity terms ( $<10\%$ ). Inside the last closed flux surface  $E_\psi$  is negative, with higher values in H-mode compared to L-mode. The change in the radial electric field, referred to that in the first L-mode period, is shown in Fig 4. The region of maximum shear  $\partial E_y / \partial r \approx 2 \times 10^3 \text{ kV/m}^2$  is located close to the 95% flux surface and evolves only after the L-H transition. As in the case of the poloidal velocity shear, the radial electric field shear starts to

$a > Rqsm_0 J_{tot} / eB(1 + sb_p)$  where  $J_{tot}$  is the total edge current density [8].  $J_{tot} = j_{Ind} + j_{BS}$  can be estimated from the surface voltage, the neoclassical resistivity and the pressure gradient, and the evolution of the edge stability to the peeling mode can be followed during a current ramp. Fig. 2 shows this for a discharge initially in dithering H-mode. The trajectory of the discharge during current ramp-down is away from the

assumed instability boundary into a region of improved peeling mode stability, as the discharge evolves from dithering H- to L-mode. Trajectories for current ramp-up are oppositely directed i.e. into regions of decreased stability during the ramp, although the discharge

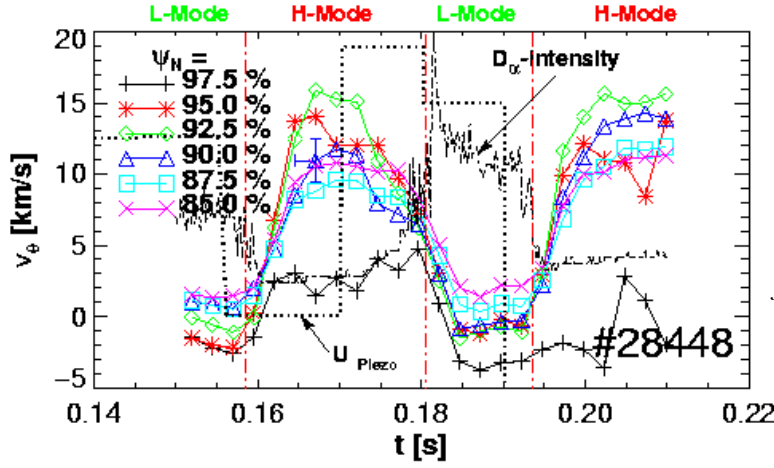


Fig.3 Time variation of the poloidal  $He^+$  velocity on different flux surfaces, together with the divertor  $D_\alpha$  emission and the gas puff control waveform. The different confinement modes of the discharge are indicated and the timing of the first L-H transition is marked by the vertical line at 0.158s.

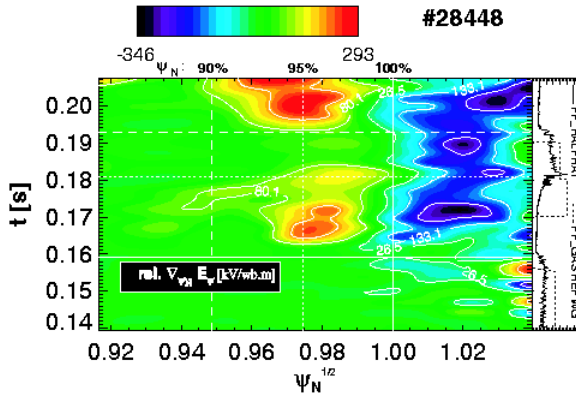


Fig.4 Evolution of the shear profile of the radial electric field referred to that in the first L-mode period. On the right hand side time traces of the  $D_\alpha$  intensity and the gas puff control waveform are shown to illustrate the different phases of the shot. Red:large +ve, blue:large -ve

dependence on density, with central electron temperature staying approximately constant.

Table 1.

|                            | #26363<br>0.147s ECH | #27907<br>0.245s OH |
|----------------------------|----------------------|---------------------|
| $q_{95}$                   | 4.6                  | 4.3                 |
| $B_T$ [T]                  | 2.07                 | 1.1                 |
| $I_p$ [kA]                 | 242                  | 140                 |
| $n_{19}$                   | 5.1                  | 5.4                 |
| $P$ [MW] <sub>40%abs</sub> | 0.34                 | 0.18                |
| $W$ [kJ]                   | 4.9                  | 2.2                 |
| $T_c(0)$ [keV]             | 1.4                  | 0.66                |
| $f_{ELM}/f_{ST}$ [Hz]      | 500/350              | 400/650             |
| $\beta_N$                  | 0.58                 | 0.80                |
| $v^*$ [a.u.]               | 4.5                  | 24                  |
| $\rho^*$ [a.u.]            | 9.6                  | 12                  |
| $\chi^*$ [a.u.]            | 10                   | 15                  |

Table 1. Comparison of parameters in two COMPASS-D ELMy H-mode shots differing by factor  $\sim 5$  in  $r^*$

The data are consistent with weak dependence of the dimensionless thermal diffusivity

decay before the H-L transition and rapidly

( $\sim 2.5$ ms) reduces to the previous L-mode value. The region of maximum electric field shear correlates with the maximum electron pressure gradient, which defines the transport barrier.

#### 4. Stationary ELMy H-mode discharges

Stationary ELMy H-mode discharges can be obtained on COMPASS-D, with on-axis ECRH, albeit in a relatively restricted operational window limited to densities above  $\bar{n}_e \sim 3.6 \times 10^{19} \text{m}^{-3}$  and launched  $P_{ECRH}$  greater than  $\sim 0.5$  MW [12]. The stationary phase can last for the whole of the heating pulse. The energy content shows a roughly linear

Correcting for  $\sim 40\%$  ECRH absorption efficiency at  $\bar{n}_e = 5 \times 10^{19} \text{m}^{-3}$ , (estimated from experiment and ray-tracing), the energy confinement is equivalent to  $H_H \approx 0.8$ , relative to ELMy H-mode scaling [13]. Note that over the full range of density, and for both Ohmic and ECRH heated plasmas, ITER scalings predict only a small improvement across the L-H transition for the same engineering parameters:  $\tau_{E,ITERH}/\tau_{E,ITERL} = 1.1-1.2$ . Data from these plasmas and from Ohmically heated ELMy H-mode plasmas have been used to test the collisionality dependence of the energy confinement. Table 1 shows parameters from 2 such shots differing by a factor 5.3 in volume-averaged collisionality  $v^*$ , with only small differences in other dimensionless parameters.

$\chi^* \equiv \tau_{Bohm} / \tau_E$  on  $v^*$ , in agreement with the International Confinement Database and other single machine scans. ELMy H-mode discharges have been achieved on COMPASS-D down to  $q_{95}$  values of 2.6 with no significant degradation in normalised confinement.

## 5. Summary

High resolution measurements in the region of the H-mode transport barrier on COMPASS-D enable the behaviour of derived normalised local parameters to be compared with a variety of transition theories/models. Four examples of these are shown to have stability regimes whose limiting boundaries are not inconsistent with the experimental L-H transition boundaries. This suggests that all the turbulence mechanisms involved may have to be stabilised for the H-mode to be initiated, but does not identify which mechanism controls the transition. Experiments using current ramps to trigger transitions (by varying the drive term of the peeling mode instability) in low density ECRH H-modes, where COMPASS-D power thresholds are markedly different from ITER scalings, show that the peeling mode does not appear to be the controlling mechanism in this regime. A transition theory based on Alfvén-drift wave turbulence suppression is attractive because it exhibits pre-cursor behaviour in the stability regime diagram, and gives density and magnetic field dependencies in agreement both with the very different global power scalings observed on COMPASS-D, and with the ITER scalings.

Detailed measurements of the evolution of the poloidal velocity and associated radial electric field throughout periods of L and H-mode have shown that significant shear develops only after the L-H transition. This is in contrast to observations recorded on some other devices, and may be linked with the different trigger mechanisms which control the transition in different regimes. In triggered H-L transitions, reduction in shear occurs before the back-transition, which takes place when the shear has regained its L-mode value.

COMPASS-D produces quasi-stationary ELMy H-modes with ECRH. These plasmas provide valuable confinement data in the regime where heat is deposited primarily to the electrons. An intra-machine factor-of-five collisionality scan has been undertaken and results show a weak-positive dependence of thermal diffusivity in agreement with the ITER database and single machine scans. Normalised confinement does not significantly degrade in these discharges down to  $q_{95} \sim 2.6$ .

## References

- [1] A.R.Field, N.J.Conway, P.G.Carolan, M.G.O'Mullane, *Rev Sci Inst*, **70**, No 1 (1999)
- [2] S.J.Fielding et al 25<sup>th</sup> EPS Conf Cont Fus & Plasma Phys (Prague, Czech Rep 1998) B092
- [3] JW Connor, RJ Hastie, HR Wilson, RL Miller, *Phys Plasmas* **5** (1998) 2687
- [4] BN Rogers JF Drake, *Phys Rev Lett* **79** (1997) 229
- [5] P Helander *Phys Plasmas* **5** (1998) 3999
- [6] O Pogutse, Yu Ighitkhanov et al, 24<sup>th</sup> EPS, Berchtesgaden, part III (1997) 1545
- [7] S.J.Fielding et al *Plasma Phys Contr Fusion* **42** (2000) A191-A197
- [8] HRWilson et al, *Phys Plasmas* **6** (1999) 1925
- [9] S.J.Fielding et al *Plasma Phys Contr Fusion* **38** (1996) 1091
- [10] G.Huysmans 24<sup>th</sup> EPS Conf Cont Fus & Plas Phys (Berchtesgaden, Germany 1997) **21A(11)** p21
- [11] H Meyer et al, 27<sup>th</sup> EPS Conf Cont Fus & Plasma Phys (Budapest, Hungary 2000) P1-042
- [12] M Valovic et al 26<sup>th</sup> EPS Conf Cont Fus & Plasma Phys (Maastricht, Holland 1999) **23J** p149
- [13] K Thomsen *et al*, 17<sup>th</sup> IAEA Fusion Energy Conf, Yokohama (1998)

IAEA-CN-69/ITER/3-ITERP1/07

*This work is funded jointly by the UK Department of Trade and Industry and EURATOM*